

Dirac Leptogenesis in Left-Right Symmetric Models

K.S. Babu,^a Ajay Kaladharan^a

^a*Department of Physics, Oklahoma State University, Stillwater, OK 74078, USA*

E-mail: babu@okstate.edu, kaladharan.ajay@okstate.edu

ABSTRACT: Left-right symmetric models which employ a generalized seesaw mechanism to generate quark and charged lepton masses are known to solve the strong CP problem via parity symmetry, without the need for the axion. These models lead to naturally light Dirac neutrinos with their masses arising through radiative corrections. In this work, we show how baryogenesis via Dirac leptogenesis can be implemented in this framework. A pair of left-right symmetric scalar doublets $\phi_{L,R}$ carrying $(B - L)$ charge of 3 is introduced for this purpose, which preserves the parity solution to the strong CP problem. Small neutrino masses are generated through one-loop diagrams mediated by these scalars. The decay of vector-like leptons (E_i) involved in the seesaw mechanism to generate charged lepton masses, $E_i \rightarrow \bar{\nu}_{jR} \phi_{R}^-$, creates a right-handed neutrino (ν_R) asymmetry, while preserving total lepton number. The compensating lepton asymmetry is converted to baryon asymmetry via electroweak sphalerons. We show that for a large range of model parameters successful baryogenesis can be realized, with the W_R^\pm gauge boson mass being as low as 10^6 GeV.

Contents

1	Introduction	1
2	The Model	3
3	Loop-Induced Dirac Neutrino Masses	7
4	Dirac Leptogenesis	9
4.1	Results	14
5	Resonant Leptogenesis	15
6	Summary	18
A	Yukawa Matrices for benchmark points	18
A.1	Non-resonant leptogenesis	18
A.2	Resonant leptogenesis	20

1 Introduction

The Standard Model (SM) has been remarkably successful in explaining the fundamental forces of nature, but it falls short in explaining the matter-antimatter asymmetry [1] of the Universe as well as the experimentally observed neutrino oscillation data [2–5] which require neutrinos to have small but non-vanishing masses. The oscillation data, however, cannot differentiate between the Dirac nature and the Majorana nature of neutrinos. If the neutrino is a Dirac particles, lepton number (L) would be a conserved symmetry, while for a Majorana neutrino L is broken by two units. Observation of neutrinoless double beta decay, which violates L by two units, would confirm the Majorana nature of neutrinos (for a review of the current status, see Ref. [6]). However, this process, or any other L -violating process has not been observed thus far, and the Dirac/Majorana nature of the neutrino remains an experimentally unsettled question.

In the case of Majorana neutrinos the seesaw mechanism [7–11] involving right-handed neutrinos (ν_R) explains the smallness of neutrino mass elegantly. The same ν_R fields can be responsible for the baryon asymmetry of the Universe, as their decays into leptons and the Higgs doublet of the SM can generate an asymmetry in lepton number (“leptogenesis”) [12], which is converted to baryon asymmetry by the non-perturbative sphaleron interactions of the electroweak sector [13]. (For a review see, for e.g, Ref. [14].) Thus, two of the missing ingredients of the SM, viz., small but non-zero neutrino masses and a mechanism to create the baryon asymmetry of the Universe are solved with one stroke in this setup.

There is a similar, although less studied, mechanism for baryon asymmetry generation if the neutrinos are Dirac particles. In this ‘‘Dirac leptogenesis’’ mechanism [15], an asymmetry in ν_R number is created at high temperatures in the early history of the Universe, without breaking lepton number. This asymmetry survives down to low temperatures, since the ν_R fields remain out of equilibrium with the SM plasma. The ν_R ’s, being singlets of the SM, interact with the plasma only through their tiny Yukawa couplings, which are too weak (given the smallness of the neutrino mass) to maintain equilibrium. Since lepton number L is conserved, an equal and opposite asymmetry is created in the SM sector, which is converted to baryon asymmetry by the electroweak sphaleron interactions. For realistic models that realize this mechanism in various extensions of the SM, see Ref. [16–27]. Thus, this setup also solves the two shortcomings (small neutrino mass and baryon asymmetry) of the SM with a single stroke. One difference, however, compared to the Majorana leptogenesis is that the smallness of the neutrino mass is not always guaranteed in the case of Dirac neutrinos. The purpose of this paper is propose and analyze Dirac leptogenesis in a class of left-right symmetric models where the neutrinos are naturally light Dirac particles with their small masses arising from radiative corrections.

Left-right symmetric models (LRSM) based on the gauge group $SU(3)_c \otimes SU(2)_L \otimes SU(2)_R \otimes U(1)_{B-L}$ [28–32] are well-motivated extensions of the SM, since they provide a dynamical understanding of the origin of parity violation. These models require the existence of the right-handed neutrino ν_R as the $SU(2)_R$ -partner of the right-handed electron (e_R) field, which makes them an excellent framework to address neutrino masses and their Majorana versus Dirac nature. In a class of left-right symmetric models employing a simple Higgs sector consisting of a pair of $SU(2)_{L,R}$ doublets, the masses of quarks and charged leptons arise through a generalized seesaw mechanism involving vector-like fermions [33–37]. In this class of models it is natural for the neutrino to be a Dirac particle, as its mass is zero at the tree-level, with small masses arising through loop diagrams [38–40]. The matter spectrum of the model fits in precisely in the simplest left-right symmetric $SU(5)_L \otimes SU(5)_R$ unified theory [41]. The focus of this paper is the realization of Dirac leptogenesis in this class of models. A ν_R asymmetry is created at high temperatures in the early history of the Universe in the decay of the vector-like lepton E_i involved in the charged lepton mass generation, which survives down to low temperatures, and is converted first to SM lepton asymmetry and then to baryon asymmetry by the electroweak sphalerons.

This class of models has an added benefit in that it also provides a solution to the strong CP problem with parity symmetry, without the need for the axion [37]. The θ parameter of QCD is zero due to parity, and the structure of the quark mass matrix is such that the flavor contribution to $\bar{\theta}$ is also zero at tree-level as well as one-loop level. The two-loop induced $\bar{\theta}$ is naturally small and consistent with neutron electric dipole moment constraints [37, 42, 43]. These models have been extensively studied in the recent literature in the context of flavor physics [44–47], neutrino oscillations [41, 48, 49] and gravitational wave detection [50]. The model we propose is an extension of the minimal model of Ref. [37] with the addition of a pair of $SU(2)_{L,R}$ Higgs doublets carrying $(B - L)$ charge of 3, which serves two purposes. These scalars contribute to one-loop neutrino mass generation and also enable a mechanism to generate ν_R asymmetry in the early universe.

The rest of the paper is organized as follows. In the [Sec. 2](#), we introduce the details of the model and follow it with the neutrino mass mechanism in the [Sec. 3](#). In [Sec. 4](#), we explain the Dirac leptogenesis mechanism in the model and provide the relevant Boltzmann equations. In [Sec. 5](#), we study the special case of resonant leptogenesis as applied to the model. Finally, in the [Sec. 6](#), we summarize our main results. [Appendix A](#) provides the numerical values of the relevant Yukawa matrices and bare mass matrices for the benchmark points that we have presented.

2 The Model

Left-right symmetric models are based on the gauge symmetry $SU(3)_c \otimes SU(2)_L \otimes SU(2)_R \otimes SU(2)_{B-L}$ [28–32]. The standard model fermions, along with the right-handed neutrino, form doublets under this gauge group in a left-right symmetric manner ($i = 1 - 3$ is the family index):

$$\begin{aligned} Q_{L,i} \left(3, 2, 1, +\frac{1}{3} \right) &\equiv \begin{pmatrix} u_L \\ d_L \end{pmatrix}_i, & Q_{R,i} \left(3, 1, 2, +\frac{1}{3} \right) &\equiv \begin{pmatrix} u_R \\ d_R \end{pmatrix}_i, \\ \psi_{L,i} (1, 2, 1, -1) &\equiv \begin{pmatrix} \nu_L \\ e_L \end{pmatrix}_i, & \psi_{R,i} (1, 1, 2, -1) &\equiv \begin{pmatrix} \nu_R \\ e_R \end{pmatrix}_i. \end{aligned} \quad (2.1)$$

Three families of vector-like fermions, which are singlets under $SU(2)_L \otimes SU(2)_R$, are introduced in the model to generate masses for the usual fermion via a generalized seesaw mechanism [33–37]:

$$E_{L/R}(1, 1, 1, -2), \quad U_{L/R}(3, 1, 1, \frac{4}{3}), \quad D_{L/R}(3, 1, 1, -\frac{2}{3}). \quad (2.2)$$

The specific version of this class of left-right symmetric model that we propose for small Dirac neutrino masses as well as Dirac leptogenesis has the following Higgs fields:

$$\begin{aligned} \chi_L (1, 2, 1, 1) &\equiv \begin{pmatrix} \chi_L^+ \\ \chi_L^0 \end{pmatrix}, & \chi_R (1, 1, 2, 1) &\equiv \begin{pmatrix} \chi_R^+ \\ \chi_R^0 \end{pmatrix}, \\ \phi_L (1, 2, 1, 3) &\equiv \begin{pmatrix} \phi_L^{++} \\ \phi_L^+ \end{pmatrix}, & \phi_R (1, 1, 2, 3) &\equiv \begin{pmatrix} \phi_R^{++} \\ \phi_R^+ \end{pmatrix}. \end{aligned} \quad (2.3)$$

The fields $\chi_{L,R}$ are employed to break the gauge symmetry down to $SU(3)_c \otimes U(1)_{\text{em}}$. This spontaneous symmetry breaking occurs in two steps: $SU(3)_c \otimes SU(2)_L \otimes SU(2)_R \otimes U(1)_{B-L} \rightarrow SU(3)_C \otimes SU(2)_L \otimes U(1)_Y \rightarrow SU(3)_c \otimes U(1)_{\text{em}}$, via vacuum expectation values (VEVs) of the neutral components of χ_R and χ_L given by

$$\langle \chi_L^0 \rangle = \kappa_L, \quad \langle \chi_R^0 \rangle = \kappa_R, \quad (2.4)$$

with the hierarchy $\kappa_R \gg \kappa_L = 174 \text{ GeV}$. The $(B - L) = 3$ scalar fields $\phi_{L,R}$ are used to generate small Dirac neutrino masses via one-loop Feynman diagrams. They also enable the creation of ν_R asymmetry in the early universe via the decay $E_i \rightarrow \bar{\nu}_{Rj} \phi_R^-$. It should be

noted that small Dirac neutrino masses can be induced in the model via the exchange of a singlet charged scalar (rather than the pair of doublets $\phi_{L,R}$ of Eq. (2.3) [49]). But in such a scenario, we found that it is difficult to explain baryon asymmetry via Dirac leptogenesis and neutrino oscillation data simultaneously. In Ref. [48], a second pair of doublet scalars $\chi'_{L,R}$ fields with a $(B - L)$ charge of 1 was proposed to generate Dirac neutrino masses through the exchange of the physical charged Higgs bosons. In that scenario, however, the fact that both doublets have neutral components acquiring VEVs, which are complex in general, would spoil the strong CP solution via parity symmetry (the determinant of the quark mass matrix will no longer be real). Our choice of $\phi_{L,R}$ doublets as shown in Eq. (2.3) avoids this problem, as there are no neutral components in these fields that acquire VEVs. Furthermore, these $\phi_{L,R}$ fields do not couple to the quarks at all, and the parity solution to the strong CP problem is preserved as in the minimal model [37]. The exchange of $\phi_{R,L}^-$ fields generate small Dirac neutrino masses via one-loop diagrams in our model.¹ The couplings of $\phi_{L,R}$ fields to the leptons is such that lepton number remains conserved, which can be seen by assigning $L = 2$ to $\phi_{L,R}$. (This will become clear from the Yukawa interactions discussed later in this section.) Owing to this lepton number symmetry $\phi_{L,R}^\pm$ do not mix with the $\chi_{L,R}^\pm$ fields which carry $L = 0$ and are in fact the Goldstone bosons eaten by the $W_{L,R}^\pm$ gauge bosons.

The general Higgs potential involving the $\chi_{L,R}$ and $\phi_{L,R}$ fields is given by

$$\begin{aligned}
V = & -\mu_L^2 \chi_L^\dagger \chi_L + \mu_R^2 \chi_R^\dagger \chi_R + m_L^2 \phi_L^\dagger \phi_L + m_R^2 \phi_R^\dagger \phi_R + \frac{\lambda_1}{2} \left((\chi_L^\dagger \chi_L)^2 + (\chi_R^\dagger \chi_R)^2 \right) \\
& + \lambda_2 (\chi_L^\dagger \chi_L)(\chi_R^\dagger \chi_R) + \frac{\lambda_3}{2} \left((\phi_L^\dagger \phi_L)^2 + (\phi_R^\dagger \phi_R)^2 \right) + \lambda_4 (\phi_L^\dagger \phi_L)(\phi_R^\dagger \phi_R) \\
& + \left\{ \lambda_5 (\chi_L^\dagger \phi_L)(\phi_R^\dagger \chi_R) + \text{h.c.} \right\} + \lambda_6 \left((\chi_L^\dagger \chi_L)(\phi_L^\dagger \phi_L) + (\chi_R^\dagger \chi_R)(\phi_R^\dagger \phi_R) \right) \\
& + \lambda_7 \left((\chi_L^\dagger \phi_L)(\phi_L^\dagger \chi_L) + (\chi_R^\dagger \phi_R)(\phi_R^\dagger \chi_R) \right) + \lambda_8 \left((\chi_L^\dagger \chi_L)(\phi_R^\dagger \phi_R) + (\chi_R^\dagger \chi_R)(\phi_L^\dagger \phi_L) \right).
\end{aligned} \tag{2.5}$$

Here we have imposed parity symmetry under which $\chi_L \leftrightarrow \chi_R$ and $\phi_L \leftrightarrow \phi_R$, but we have allowed for its soft breaking by the quadratic mass terms for these fields.

The 2×2 mass matrix for the neutral scalar fields $\sigma_{L/R} = \text{Re}(\chi_{L/R}^0)$ is given by

$$\mathcal{M}_{\sigma_{L,R}} = \begin{bmatrix} 2\lambda_1 \kappa_L^2 & 2\lambda_2 \kappa_L \kappa_R \\ 2\lambda_2 \kappa_L \kappa_R & 2\lambda_1 \kappa_R^2 \end{bmatrix}. \tag{2.6}$$

The lightest mass eigenstate (of mass M_h) is identified as the Standard Model Higgs h of mass 125 GeV, while H denotes a heavier scalar. The mass eigenstates and the physical Higgs masses are given by ($s_x \equiv \sin x$, $c_x \equiv \cos x$)

$$h = c_\xi \sigma_L - s_\xi \sigma_R, \quad H = s_\xi \sigma_L + c_\xi \sigma_R \tag{2.7}$$

¹Ref. [51] has introduced both a singlet charged scalar and the $(B - L) = 3$ doublet scalars ϕ_{LR} to generate neutrino masses. However, we find that the singlet charged scalar is not necessary for this purpose, as shown in Sec. 3.

$$M_h^2 \simeq 2\lambda_1 \left(1 - \frac{\lambda_2^2}{\lambda_1^2}\right) \kappa_L^2, \quad M_H^2 \simeq 2\lambda_1 \kappa_R^2. \quad (2.8)$$

The mixing angle ξ is given by

$$\tan 2\xi = \frac{2\lambda_2 \kappa_L \kappa_R}{\lambda_1 \kappa_R^2 - \lambda_1 \kappa_L^2}. \quad (2.9)$$

The masses of doubly charged scalars are given by

$$M_{\phi_L^{++}}^2 = m_L^2 + \lambda_6 \kappa_L^2 + \lambda_8 \kappa_R^2, \quad (2.10)$$

$$M_{\phi_R^{++}}^2 = m_R^2 + \lambda_6 \kappa_R^2 + \lambda_8 \kappa_L^2. \quad (2.11)$$

The singly charged scalars $\phi_{L/R}^+$ mix with a mass matrix given by

$$M_{\phi_{L/R}^+}^2 = \begin{bmatrix} m_L^2 + (\lambda_6 + \lambda_7) \kappa_L^2 + \lambda_8 \kappa_R^2 & \lambda_5 \kappa_L \kappa_R \\ \lambda_5 \kappa_L \kappa_R & m_R^2 + (\lambda_6 + \lambda_7) \kappa_R^2 + \lambda_8 \kappa_L^2 \end{bmatrix}. \quad (2.12)$$

The mass eigenstates and the physical masses of these charged scalars are given by

$$h_1^\pm = c_{\theta_\pm} \phi_L^\pm - s_{\theta_\pm} \phi_R^\pm \quad (2.13)$$

$$h_2^\pm = c_{\theta_\pm} \phi_R^\pm + s_{\theta_\pm} \phi_L^\pm \quad (2.14)$$

$$M_{h_{1/2}^\pm}^2 = \frac{1}{2} \left(\mathcal{M}_{11} + \mathcal{M}_{11} \mp \sqrt{(\mathcal{M}_{22} - \mathcal{M}_{11})^2 + 4\mathcal{M}_{12}^2} \right), \quad (2.15)$$

where \mathcal{M}_{ij} denotes (i, j) element of Eq. (2.12) and the mixing angle θ_\pm is given by

$$\tan 2\theta_\pm = \frac{2\mathcal{M}_{12}}{\mathcal{M}_{22} - \mathcal{M}_{11}}, \quad (2.16)$$

It is worth noting that in the electroweak symmetric vacuum, which is realized at temperatures well above 100 GeV, the mixing angle θ_\pm vanishes and therefore the mass eigenvalues are given by the diagonal entries of Eq. (2.12), which we shall denote as $M_{\phi_L^+}^2$ and $M_{\phi_R^+}^2$, respectively.

The Yukawa couplings of fermions, along with the bare mass terms for the vector-like fermions, are given by the Lagrangian

$$\begin{aligned} \mathcal{L}_{\text{Yuk}} = & \mathcal{Y}_u \bar{Q}_L \tilde{\chi}_L U_R + \mathcal{Y}_u \bar{Q}_R \tilde{\chi}_R U_L + M_U \bar{U}_L U_R \\ & + \mathcal{Y}_d \bar{Q}_L \chi_L D_R + \mathcal{Y}_d \bar{Q}_R \chi_R D_L + M_D \bar{D}_L D_R \\ & + \mathcal{Y}_\ell \bar{\psi}_L \chi_L E_R + \mathcal{Y}_\ell \bar{\psi}_R \chi_R E_L + M_E \bar{E}_L E_R \\ & + f (\psi_{Li}^T \mathcal{C} \phi_{Lj} E_L \epsilon^{ij} + \psi_{Ri}^T \mathcal{C} \phi_{Rj} E_R \epsilon^{ij}) + \text{h.c.}, \end{aligned} \quad (2.17)$$

with $\tilde{\chi}_{L/R} = i\tau_2 \chi_{L/R}^*$ and i, j are $SU(2)_{L/R}$ indices. Under parity symmetry the fermions and scalar fields transform as

$$Q_L \leftrightarrow Q_R, \quad \psi_L \leftrightarrow \psi_R, \quad U_L \leftrightarrow U_R, \quad D_L \leftrightarrow D_R, \quad E_L \leftrightarrow E_R, \quad \chi_L \leftrightarrow \chi_R, \quad \phi_L \leftrightarrow \phi_R. \quad (2.18)$$

As a result, the vector-like fermion mass matrices $M_{U,D,E}$ are hermitian in Eq. (2.17). The Lagrangian of Eq. (2.17) generates 6×6 mass matrices for charged leptons (e , E), up-type quarks (u , U), and down-type quarks (d , D), which can be expressed in block form as

$$\mathcal{M}_f = \begin{pmatrix} 0 & \mathcal{Y}_f \kappa_L \\ \mathcal{Y}_f^\dagger \kappa_R & M_f \end{pmatrix} \quad (f = \ell, u, d). \quad (2.19)$$

It is clear from here that the determinant of the quark mass matrices are real, which helps solve the strong CP problem.

Using two unitary matrices $\mathcal{U}_{L/R}$, we can block-diagonalize matrix \mathcal{M}_f via a bi-unitary transformation, $\mathcal{U}_L^\dagger \mathcal{M}_f \mathcal{U}_R = \mathcal{M}_{\text{block}}$. Defining

$$\rho_{Lf} = \mathcal{Y}_f \kappa_L M_f^{-1}, \quad \rho_{Rf} = \mathcal{Y}_f \kappa_R M_f^{-1}, \quad (2.20)$$

we can parametrize the unitary matrices $\mathcal{U}_{L/R}$, with the assumption $\rho_{L,R} \ll 1$ as

$$\mathcal{U}_{Lf} = \begin{pmatrix} 1 - \frac{1}{2} \rho_{Lf}^\dagger \rho_{Lf} & \rho_{Lf} \\ -\rho_{Lf}^\dagger & 1 - \frac{1}{2} \rho_{Lf} \rho_{Lf}^\dagger \end{pmatrix}, \quad \mathcal{U}_{Rf} = \begin{pmatrix} 1 - \frac{1}{2} \rho_{Rf}^\dagger \rho_{Rf} & \rho_{Rf} \\ -\rho_{Rf}^\dagger & 1 - \frac{1}{2} \rho_{Rf} \rho_{Rf}^\dagger \end{pmatrix}. \quad (2.21)$$

The assumption $\rho_L \ll 1$ follows from our phenomenological requirement $\kappa_L \ll \kappa_R$, so that the W_R^\pm mass is much larger than the W_L^\pm mass. While ρ_R can be of order unity in general, to simplify our analysis, and to realize Dirac leptogenesis, we will focus on the regime with $\rho_{L,R} \ll 1$. This is because we are interested in the parameter space with M_E is of similar order as κ_R . To explain the charged lepton mass, one requires $\mathcal{Y}_\ell \ll 1$ in this case, which leads to $\rho_R \ll 1$. (For a 2×2 seesaw matrix of the form given in Eq. (2.19), the lightest eigenvalue is $m_\ell \simeq y_\ell \kappa_L \cos \theta_R^\ell$, where $\tan \theta_R^\ell = y_\ell \kappa_R / M_\ell$. When $\kappa_R \sim M_\ell$, $\cos \theta_R \sim \mathcal{O}(1)$ and to explain the charged lepton mass one would need $y_\ell \ll 1$, and hence $\rho_R \ll 1$.) We shall assume this in our numerical analysis, but we have verified that this condition holds by checking the approximate results with exact numerical results.

The 3×3 blocks of the block-diagonal matrix M_{block} are given by

$$\hat{m}_f = -\kappa_L \kappa_R \mathcal{Y}_f M_f^{-1} \mathcal{Y}_f^\dagger, \quad \hat{M}_f = M_f + \frac{1}{2} \left(\kappa_R^2 \mathcal{Y}_f^\dagger \mathcal{Y}_f M_f^{-1} + \kappa_L^2 \mathcal{Y}_f \mathcal{Y}_f^\dagger M_f^{-1} \right). \quad (2.22)$$

The hermitian matrix \hat{m}_f can be diagonalized using a unitary matrix $m_f = U_f \hat{m}_f U_f^\dagger$, while the matrix \hat{M} can be diagonalized using a bi-unitary transformation $\hat{M}_f = V_{Lf} M_f^d V_{Rf}^\dagger$, where m_f and M_f^d are the diagonal matrix. In the case when M_f is diagonal, which can be chosen without loss of generality by a flavor rotation, the Yukawa matrix \mathcal{Y}_f can be parametrized as

$$\mathcal{Y}_f = \frac{1}{\sqrt{\kappa_L \kappa_R}} U_f^\dagger m_f^{1/2} U'_f M_f^{1/2}, \quad (2.23)$$

where U'_f is general unitary matrix which can be parameterized using the standard CKM-like parameterization.

The charged gauge bosons do not undergo mixing at the tree level, and their masses are evaluated as:

$$M_{W_L^\pm}^2 = \frac{1}{2} g_L \kappa_L^2, \quad M_{W_R^\pm}^2 = \frac{1}{2} g_R \kappa_R^2. \quad (2.24)$$

For the neutral gauge boson sector, the photon field A_μ remains massless while the orthogonal fields Z_L and Z_R undergo mixing at the tree level, and the mixing matrix is given by

$$M_{Z_L-Z_R}^2 = \frac{1}{2} \begin{pmatrix} (g_L^2 + g_Y^2)\kappa_L^2 & g_Y^2 \sqrt{\frac{g_L^2 + g_Y^2}{g_R^2 - g_Y^2}} \kappa_L^2 \\ g_Y^2 \sqrt{\frac{g_L^2 + g_Y^2}{g_R^2 - g_Y^2}} \kappa_L^2 & \frac{g_R^4 \kappa_R^2 + g_Y^2 \kappa_L^2}{g_R^2 - g_Y^2} \end{pmatrix}. \quad (2.25)$$

The masses of neutral gauge bosons are given approximately by

$$M_{Z_1}^2 \simeq \frac{1}{2}(g_Y^2 + g_L^2)\kappa_L^2 \quad M_{Z_2}^2 \simeq \frac{1}{2} \frac{g_R^4 \kappa_R^2 + g_Y^2 \kappa_L^2}{g_R^2 - g_Y^2}. \quad (2.26)$$

Under the parity symmetry, the gauge boson transforms as $W_L^\pm \leftrightarrow W_R^\pm$, implying that the gauge couplings for $SU(2)_L$ and $SU(2)_R$ are equal: $g_L = g_R$ at the scale κ_R . The embedding of $U(1)_Y \subset SU(2)_R \otimes U(1)_{B-L}$ yields the matching condition for hypercharge Y and the corresponding gauge coupling g_Y ,

$$\frac{Y}{2} = T_{3R} + \frac{B-L}{2}, \quad \frac{1}{g_Y^2} = \frac{1}{g_R^2} + \frac{1}{g_B^2}. \quad (2.27)$$

These relations will be used in our numerical studies of Dirac leptogenesis.

It is important to emphasize that the neutrino masses are zero at the tree level in the model. This is partly because there is no vector-like neutral lepton with which the neutrino can mix. In fact, the vector-like fermion spectrum given in Eq. (2.2) is exactly what would arise from an embedding of the left-right theory in a parity-symmetric $SU(5)_L \otimes SU(5)_R$ unified theory, which justifies the absence of vector-like neutral leptons. The absence of tree-level neutrino mass also has to do with the absence of a bidoublet scalar used in the standard LRSM, which is not necessary in the present context of generalized seesaw for quark and charged lepton mass generation. Neutrinos will acquire small Dirac masses through loop diagrams, which we analyze in the next section.

3 Loop-Induced Dirac Neutrino Masses

In the model under study the neutrinos can be naturally light Dirac particles. As argued earlier, there is no vector-like neutral lepton that can induce the neutrino a tree-level mass. While it is possible that without additional scalar fields the neutrino would acquire small Dirac mass via a two-loop induced diagram mediated by $W_L^+ - W_R^+$ mixing [38, 39], consistent with neutrino oscillation data, that scenario does not appear to have the ingredients for successful Dirac leptogenesis. Our proposal extends the simplest model with the pair of $B - L = 3$ scalar fields $\phi_{L,R}$, which we found to be the simplest extension to accommodate Dirac leptogenesis, as well as to explain neutrino oscillation data. In this context, we shall assume that the contribution of the two-loop $W_L^\pm - W_R^\pm$ exchange diagram is small, which can be achieved, for example, by keeping the bare mass of the top partner M_{U_3} to be small, so that the loop-induced $W_L^\pm - W_R^\pm$ mixing is suppressed.

To evaluate the loop-induced Dirac neutrino masses, we work in a basis where the vector-like charged lepton mass matrix M_E is diagonal. The model conserves lepton number;

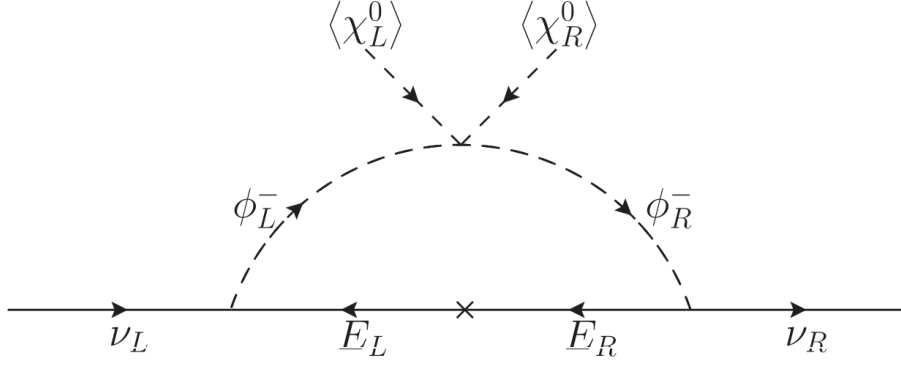


Figure 1. Diagram generating tiny Dirac neutrino masses.

the neutrinos acquire tiny Dirac masses via a one-loop mechanism arising from the diagram in the Fig. 1. The induced mass matrix can be calculated in analogy to a similar Dirac neutrino mass model analyzed in Ref. [52], following a procedure akin to that of the one-loop Majorana mass [53, 54]. The quartic coupling λ_5 induces mixing between ϕ_L^\pm and ϕ_R^\pm , with λ_5 taken to be real without loss of generality. The neutrino masses arise when both χ_L^0 and χ_R^0 acquire non-zero vacuum expectation values. In the $\rho_{R,L} \ll 1$ limit, the neutrino mass matrix can be approximated as

$$(m_\nu)_{\alpha\beta} \simeq \sum_i \left(\frac{(f_L)_{\alpha i} (f_R)_{\beta i}^* s_{2\theta_\pm}}{32\pi^2} \left[\frac{M_{E_i} M_{h_2^\pm}^2}{M_{h_2^\pm}^2 - M_{E_i}^2} \ln \left(\frac{M_{h_2^\pm}^2}{M_{E_i}^2} \right) - \frac{M_{E_i} M_{h_1^\pm}^2}{M_{h_1^\pm}^2 - M_{E_i}^2} \ln \left(\frac{M_{h_1^\pm}^2}{M_{E_i}^2} \right) \right] \right), \quad (3.1)$$

where $f_R = fV_{RE}$ and $f_L = fV_{LE}$. Here, V_{LE} and V_{RE} are the unitary transformations that diagonalizes the bare mass matrix of the heavy leptons, such that $\hat{M}_\ell = V_{LE} M_\ell^d V_{RE}^\dagger$. In the $\rho_L, \rho_R \ll 1$ limit, the matrix \hat{M}_ℓ is approximately hermitian, hence $V_{LE} \simeq V_{RE}$. In a basis where the charged lepton mass matrix is diagonal, the Dirac neutrino mass matrix takes the form

$$\tilde{m}_\nu = U_\ell m_\nu U_\ell^\dagger. \quad (3.2)$$

Subsequently, the neutrino mass matrix can be diagonalized by a unitarity transformation:

$$m_\nu^d = U^\dagger \tilde{m}_\nu U, \quad (3.3)$$

where U is the usual PMNS matrix. For a given value of $M_{h_{1,2}^\pm}$ and M_{E_i} , the Dirac neutrino masses and mixing depend on the Yukawa matrix f and the mixing angle θ_\pm . This allows enough freedom in the parameter space to provide excellent fits for the neutrino oscillation data. The smallness of the Dirac mass can be explained, for example, by choosing $f \sim \lambda_5 \sim 10^{-3}$, $\kappa_R/M_E \sim 0.1$, which would leads to an effective Dirac Yukawa coupling of order 10^{-12} . The mixing angle θ_\pm and Yukawa matrix f play a crucial role in the Dirac leptogenesis mechanism, as we discuss in the Sec. 4 later, introducing additional constraints on the parameter space. We shall present self-consistent fits to the neutrino oscillation data by also including these Dirac leptogenesis constraints in Sec. 4.

4 Dirac Leptogenesis

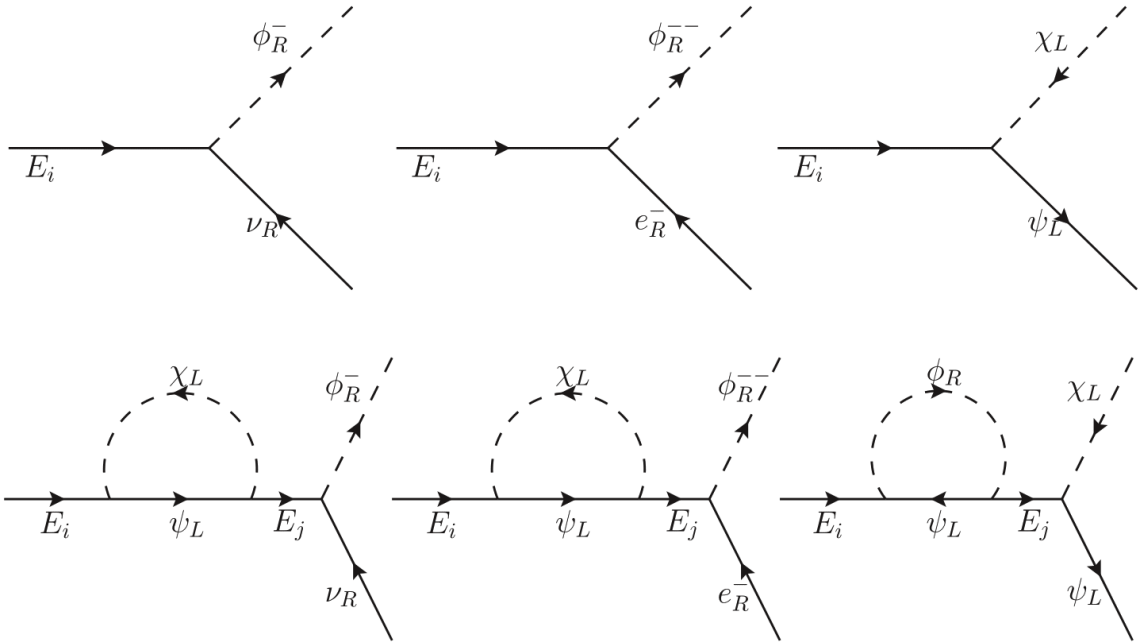


Figure 2. The tree level and one-loop wave correction for the decay of heavy Dirac state E_i to $\bar{\nu}_R\phi_R^-$, $e_R^+\phi_R^-$ and $\psi_L\bar{\chi}_L$. This diagram results in non-zero CP violation and subsequently contributes to baryon asymmetry.

In the model, Dirac leptogenesis occurs after the breaking of $SU(2)_R \otimes U(1)_{B-L}$. This leptogenesis mechanism requires a mass spectrum where $M_{E_1} > M_{\phi_R^\pm}$. The left- and right-handed massive charged leptons combine to form heavy Dirac states $E \equiv E_R + E_L$. In analogy to standard leptogenesis, the decay of the heavy Dirac state, as shown in Fig. 2, could induce the CP violation and departure from thermal equilibrium. This scenario differs from other Dirac leptogenesis models [15, 16, 19] as it occurs in two steps, described below.

In the first step, the asymmetry in ν_R is generated through the decay of the heavy Dirac state E_i :

$$E_i \rightarrow \bar{\nu}_R\phi_R^-. \quad (4.1)$$

The charged scalar ϕ_R^- carries lepton number $L = 2$. In the process of generating asymmetry in ν_R , an equal and opposite asymmetry is simultaneously produced in ϕ_R^- . To transfer this asymmetry into Standard Model leptons, ϕ_R^- must decay into ϕ_L^- , which subsequently decays into SM leptons. The second step involves the decay of ϕ_R^- , which proceeds through three channels shown in Fig. 3: the two body decays $\phi_R^- \rightarrow \phi_L^-\bar{\chi}_L^0$, $\phi_R^- \rightarrow \nu_R e_R^-$ and the three-body decay $\phi_R^- \rightarrow \nu_R\psi_L\bar{\chi}_L$. To transfer the asymmetry into Standard Model leptons, the decay $\phi_R^- \rightarrow \phi_L^-\bar{\chi}_L^0$ must remain in equilibrium, while the other two channels should be out-of-equilibrium at $T \sim M_{\phi_R^-}$. Additionally, ϕ_L^- must decay into SM fermions before electroweak symmetry breaking. Due to the smallness of the Dirac neutrino mass, the

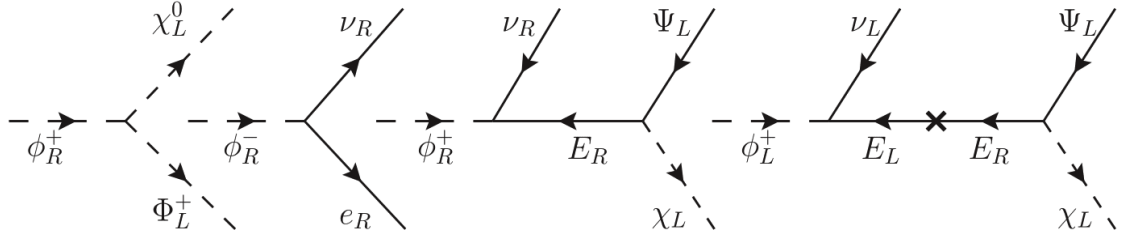


Figure 3. The decay channel for the charged scalars ϕ_L^+ and ϕ_R^+ .

asymmetry in ν_R is preserved, which in turn ensures the preservation of asymmetry in the Standard Model leptons, consistent with lepton number conservation.

The total decay width of the Dirac states E_i can be defined by

$$\Gamma(E_i) \equiv \Gamma_i = \sum_{\alpha} \left(\Gamma(E_i \rightarrow \bar{\nu}_{R\alpha} \phi_R^-) + \Gamma(E_i \rightarrow \bar{e}_{R\alpha} \phi_R^-) + \Gamma(E_i \rightarrow \bar{\psi}_{L\alpha} \phi_L) + \Gamma(E_i \rightarrow \psi_{L\alpha} \bar{\chi}_L) \right), \quad (4.2)$$

$$\Gamma_i = \frac{M_{E_i}}{16\pi} \left((f_L^\dagger f_L)_{ii} + (f_R^\dagger f_R)_{ii} + (\mathcal{Y}_L^\dagger \mathcal{Y}_L)_{ii} \right), \quad (4.3)$$

where $\mathcal{Y}_L = \mathcal{Y}_\ell V_{LE}$ and we assumed scalar particle masses are much less than M_{E_i} . The tree-level branching ratios of the heavy lepton decaying into various channels are given by:

$$\text{Br}_{\bar{\nu}_R \phi_R^-}^i = \frac{\Gamma(E_i \rightarrow \bar{\nu}_{R\alpha} \phi_R^-)}{\Gamma_i} = \frac{(f_R^\dagger f_R)_{ii}}{2(f_R^\dagger f_R)_{ii} + 2(f_L^\dagger f_L)_{ii} + 2(\mathcal{Y}_L^\dagger \mathcal{Y}_L)_{ii}} \quad (4.4)$$

$$\text{Br}_{\bar{e}_R \phi_R^-}^i = \frac{\Gamma(E_i \rightarrow \bar{e}_{R\alpha} \phi_R^-)}{\Gamma_i} = \frac{(f_R^\dagger f_R)_{ii}}{2(f_R^\dagger f_R)_{ii} + 2(f_L^\dagger f_L)_{ii} + 2(\mathcal{Y}_L^\dagger \mathcal{Y}_L)_{ii}} \quad (4.5)$$

$$\text{Br}_{\bar{\psi}_L \phi_L}^i = \frac{\Gamma(E_i \rightarrow \bar{\psi}_{L\alpha} \phi_L)}{\Gamma_i} = \frac{2(f_L^\dagger f_L)_{ii}}{2(f_R^\dagger f_R)_{ii} + 2(f_L^\dagger f_L)_{ii} + 2(\mathcal{Y}_L^\dagger \mathcal{Y}_L)_{ii}} \quad (4.6)$$

$$\text{Br}_{\psi_L \bar{\chi}_L}^i = \frac{\Gamma(E_i \rightarrow \psi_{L\alpha} \bar{\chi}_L)}{\Gamma_i} = \frac{2(\mathcal{Y}_L^\dagger \mathcal{Y}_L)_{ii}}{2(f_R^\dagger f_R)_{ii} + 2(f_L^\dagger f_L)_{ii} + 2(\mathcal{Y}_L^\dagger \mathcal{Y}_L)_{ii}} \quad (4.7)$$

The CP asymmetry associated with the process $E_i \rightarrow XY$ is defined as,

$$\epsilon_{XY}^i = \frac{\Gamma(E_i^- \rightarrow XY) - \Gamma(\bar{E}_i^+ \rightarrow \bar{X}\bar{Y})}{2\Gamma_i}. \quad (4.8)$$

Due to the CPT invariance, the decay width of Dirac state E_i and its conjugate are equal: $\Gamma_i = \bar{\Gamma}_i$. As a consequence, the sum of CP asymmetry due to the decay of E_i vanishes:

$$\epsilon_{\bar{\nu}_R \phi_R^-}^i + \epsilon_{\bar{e}_R \phi_R^-}^i + \epsilon_{\bar{\psi}_L \phi_L}^i + \epsilon_{\psi_L \bar{\chi}_L}^i = 0. \quad (4.9)$$

The diagrams responsible for the CP violation are provided in [Fig. 2](#). There is no CP violation in the $\bar{\psi}_L \phi_L$ decay channel. The one-loop diagram with amplitude proportional to f^2 and \mathcal{Y}_ℓ^2 does not lead to CP asymmetry, as summing over flavor indices cancels out CP

violation in these diagrams. The CP asymmetries generated by the decay of heavy Dirac state E_i is given by:

$$\epsilon_{\bar{\nu}_R \phi_R^-}^i = \frac{1}{8\pi} \frac{1}{(f_L^\dagger f_L)_{ii} + (f_R^\dagger f_R)_{ii} + (\mathcal{Y}_L^\dagger \mathcal{Y}_L)_{ii}} \sum_{k \neq i} \left(\frac{M_{E_i}^2}{M_{E_i}^2 - M_{E_k}^2} \text{Im} \left[(f_R^\dagger f_R)_{ki} (\mathcal{Y}_L^\dagger \mathcal{Y}_L)_{ik} \right] \right), \quad (4.10)$$

$$\epsilon_{e_R^+ \phi_R^-}^i = \frac{1}{8\pi} \frac{1}{(f_L^\dagger f_L)_{ii} + (f_R^\dagger f_R)_{ii} + (\mathcal{Y}_L^\dagger \mathcal{Y}_L)_{ii}} \sum_{k \neq i} \left(\frac{M_{E_i}^2}{M_{E_i}^2 - M_{E_k}^2} \text{Im} \left[(f_R^\dagger f_R)_{ki} (\mathcal{Y}_L^\dagger \mathcal{Y}_L)_{ik} \right] \right), \quad (4.11)$$

$$\epsilon_{\psi_L \bar{\chi}_L}^i = \frac{1}{8\pi} \frac{2}{(f_L^\dagger f_L)_{ii} + (f_R^\dagger f_R)_{ii} + (\mathcal{Y}_L^\dagger \mathcal{Y}_L)_{ii}} \sum_{k \neq i} \left(\frac{M_{E_i}^2}{M_{E_i}^2 - M_{E_k}^2} \text{Im} \left[(\mathcal{Y}_L^\dagger \mathcal{Y}_L)_{ki} (f_R^\dagger f_R)_{ik} \right] \right). \quad (4.12)$$

The Boltzmann equations which track the evolution of the asymmetries and the number densities are given by [19, 26]:

$$sH z \frac{dY_{\Sigma E_1}}{dz} = -\gamma_1 \left(\frac{Y_{\Sigma E_1}}{Y_{E_1}^{\text{eq}}} - 2 \left\{ 1 + \left[\frac{Y_{\Sigma \nu_R}}{2Y_{\nu_R}^{\text{eq}}} - 1 \right] \text{Br}_{1R} \right\} \right), \quad (4.13)$$

$$\begin{aligned} sH z \frac{dY_{\Delta E_1}}{dz} = & -\epsilon_{\bar{\nu}_R \phi_R^-}^1 \gamma_1 \left(\frac{Y_{\Sigma \nu_R}}{Y_{\nu_R}^{\text{eq}}} - 2 \right) + \gamma_1 \text{Br}_{\bar{\nu}_R \phi_R^-}^1 \left(-\frac{Y_{\Delta E_1}}{Y_{E_1}^{\text{eq}}} - \frac{Y_{\Delta \nu_R}}{Y_{\nu_R}^{\text{eq}}} + \frac{Y_{\Sigma \nu_R}}{2Y_{\nu_R}^{\text{eq}}} \frac{Y_{\Delta \phi_R^-}}{Y_{\phi_R^-}^{\text{eq}}} \right) \\ & + \gamma_1 \text{Br}_{e_R^+ \phi_R^-}^1 \left(-\frac{Y_{\Delta E_1}}{Y_{E_1}^{\text{eq}}} - \frac{Y_{\Delta e_R^-}}{Y_{e_R^-}^{\text{eq}}} + \frac{Y_{\Delta \phi_R^-}}{Y_{\phi_R^-}^{\text{eq}}} \right) + \gamma_1 \text{Br}_{\psi_L \bar{\chi}_L}^1 \left(-\frac{Y_{\Delta E_1}}{Y_{E_1}^{\text{eq}}} + \frac{Y_{\Delta \psi_L}}{Y_{\psi_L}^{\text{eq}}} \right) \\ & + \gamma_1 \text{Br}_{\psi_L \phi_L}^1 \left(-\frac{Y_{\Delta E_1}}{Y_{E_1}^{\text{eq}}} - \frac{Y_{\Delta \psi_L}}{Y_{\psi_L}^{\text{eq}}} + \frac{Y_{\Delta \phi_L}}{Y_{\phi_L}^{\text{eq}}} \right) \end{aligned} \quad (4.14)$$

$$sH z \frac{dY_{\Sigma \nu_R}}{dz} = \gamma_1 \text{Br}_{1R} \left(\frac{Y_{\Sigma E_1}}{Y_{E_1}^{\text{eq}}} - \frac{Y_{\Sigma \nu_R}}{Y_{\nu_R}^{\text{eq}}} \right) \quad (4.15)$$

$$\begin{aligned} sH z \frac{dY_{\Delta \nu_R}}{dz} = & -\epsilon_{\bar{\nu}_R \phi_R^-}^1 \gamma_1 \left(\frac{Y_{\Sigma E_1}}{Y_{E_1}^{\text{eq}}} - 2 \left\{ 1 + \left[\frac{Y_{\Sigma \nu_R}}{2Y_{\nu_R}^{\text{eq}}} - 1 \right] \text{Br}_{\bar{\nu}_R \phi_R^-}^1 \right\} \right) \\ & - \gamma_1 \text{Br}_{\bar{\nu}_R \phi_R^-}^1 \left(\frac{Y_{\Delta \nu_R}}{Y_{\nu_R}^{\text{eq}}} - \frac{Y_{\Sigma \nu_R}}{2Y_{\nu_R}^{\text{eq}}} \frac{Y_{\Delta \phi_R^-}}{Y_{\phi_R^-}^{\text{eq}}} + \frac{Y_{\Delta E_1}}{Y_{E_1}^{\text{eq}}} \right) \end{aligned} \quad (4.16)$$

$$sH z \frac{dY_{\Delta \phi_R^-}}{dz} = -sH z \frac{dY_{\Delta \nu_R}}{dz} \quad (4.17)$$

$$\begin{aligned} sH z \frac{dY_{\Delta e_R^-}}{dz} = & -\epsilon_{e_R^+ \phi_R^-}^1 \gamma_1 \left(\frac{Y_{\Sigma E_1}}{Y_{E_1}^{\text{eq}}} - 2 \left\{ 1 + \left[\frac{Y_{\Sigma \nu_R}}{2Y_{\nu_R}^{\text{eq}}} - 1 \right] \text{Br}_{\bar{\nu}_R \phi_R^-}^1 \right\} \right) \\ & - \gamma_1 \text{Br}_{e_R^+ \phi_R^-}^1 \left(\frac{Y_{\Delta e_R^-}}{Y_{e_R^-}^{\text{eq}}} - \frac{Y_{\Delta \phi_R^-}}{Y_{\phi_R^-}^{\text{eq}}} + \frac{Y_{\Delta E_1}}{Y_{E_1}^{\text{eq}}} \right) \end{aligned} \quad (4.18)$$

$$sHz \frac{dY_{\Delta\phi_R^-}}{dz} = -sHz \frac{dY_{\Delta e_R^-}}{dz} \quad (4.19)$$

$$sHz \frac{dY_{\Delta\psi_L}}{dz} = \epsilon_{\psi_L \bar{\chi}_L}^1 \gamma_1 \left(\frac{Y_{\Sigma E_1}}{Y_{E_1}^{\text{eq}}} - 2 \left\{ 1 + \left[\frac{Y_{\Sigma\nu_R}}{2Y_{\nu_R}^{\text{eq}}} - 1 \right] \text{Br}_{\nu_R \phi_R^-}^1 \right\} \right) \\ - \gamma_1 \text{Br}_{\psi_L \bar{\chi}_L}^1 \left(\frac{Y_{\Delta\psi_L}}{Y_{\psi_L}^{\text{eq}}} - \frac{Y_{\Delta E_1}}{Y_{E_1}^{\text{eq}}} \right) - \gamma_1 \text{Br}_{\psi_L \phi_L}^1 \left(\frac{Y_{\Delta\psi_L}}{Y_{\psi_L}^{\text{eq}}} - \frac{Y_{\Delta\phi_L}}{Y_{\phi_L}^{\text{eq}}} + \frac{Y_{\Delta E_1}}{Y_{E_1}^{\text{eq}}} \right) \quad (4.20)$$

$$sHz \frac{dY_{\Delta\phi_L}}{dz} = \gamma_1 \text{Br}_{\psi_L \phi_L}^1 \left(\frac{Y_{\Delta\psi_L}}{Y_{\psi_L}^{\text{eq}}} - \frac{Y_{\Delta\phi_L}}{Y_{\phi_L}^{\text{eq}}} + \frac{Y_{\Delta E_1}}{Y_{E_1}^{\text{eq}}} \right) \quad (4.21)$$

where $z \equiv M_{E_1}/T$, $Y_i = n_i/s$ with n_i number density of particle of i , $Y_{\Sigma E_1} \equiv Y_E + Y_{\bar{E}}$, $Y_{\Sigma\nu_R} \equiv Y_{\nu_R} + Y_{\bar{\nu}_R}$, $s = \frac{g_* 2\pi^2}{45} T^3$ is the entropy density, and $H = 1.66\sqrt{g_*} \frac{T^2}{M_{\text{pl}}}$ is the Hubble expansion rate with $M_{\text{pl}} = 1.22 \times 10^{19}$ GeV. The equilibrium number density Y_i^{eq} of particles of species i with mass m_i is given by,

$$Y_i^{\text{eq}} = \begin{cases} \frac{45g_i}{4\pi^4 g_*} z_i^2 \mathcal{K}_2(z_i) & z_i = \frac{m_i}{T} \neq 0 \\ \frac{15g_i \zeta_i}{8\pi^2 g_*} & m_i = 0, \end{cases} \quad (4.22)$$

where $\zeta_i = 1(2)$ for relativistic fermions (bosons) and, $\mathcal{K}_n(x)$ are modified Bessel's function. The total decay density reaction rate of E_i is given by

$$\gamma_i = s Y_{E_i}^{\text{eq}} \Gamma_i \frac{\mathcal{K}_1(z)}{\mathcal{K}_2(z)}. \quad (4.23)$$

Following the decay of the heavy vector-like lepton, an equal and opposite asymmetry develops in ν_R and ϕ_R^- . Once the ν_R asymmetry is generated, the right-handed neutrinos decouple from the Standard Model plasma, provided the ϕ_R^- decay involving ν_R is out-of-equilibrium. While the decay of ϕ_R^- into ν_R cancels the ν_R asymmetry, the two-body decay $\phi_R^- \rightarrow \phi_L^- \bar{\chi}_L^0$ preserves it. Subsequently, ϕ_L^- decays into left-handed leptons, transferring the ϕ_R^- asymmetry to the SM leptons. The width for the decay of ϕ_L^- and ϕ_R^- are given by:

$$\Gamma(\phi_R^- \rightarrow \nu_R \psi_L \bar{\chi}_L) = \sum_i \left(\frac{\sum_{\alpha\beta} |f_{\alpha i}|^2 |\mathcal{Y}_{\ell\beta i}|^2}{32\pi^3} \frac{11}{1920} \frac{M_{\phi_R^-}^5}{M_{E_i}^4} \right), \quad (4.24)$$

$$\Gamma(\phi_R^- \rightarrow \phi_L^- \bar{\chi}_L^0) = \frac{\lambda_3^2 \kappa_R^2}{16\pi^2 M_{\phi_R^-}} \left(1 - \frac{M_{\phi_L^-}^2}{M_{\phi_R^-}^2} \right), \quad (4.25)$$

$$\Gamma(\phi_L^- \rightarrow \nu_L \psi_L \bar{\chi}_L) = \sum_i \left(\frac{\sum_{\alpha\beta} |f_{\alpha i}|^2 |\mathcal{Y}_{\ell\beta i}|^2}{128\pi^3} \frac{5}{192} \frac{M_{\phi_L^-}^3}{M_{E_i}^2} \right), \quad (4.26)$$

$$\Gamma(\phi_R^- \rightarrow e_R^- + \nu_R) = \frac{\text{Tr} [f \rho_R^\dagger \rho_R f^\dagger]}{8\pi} M_{\phi_R^-}. \quad (4.27)$$

In the parameter space of interest, the three-body decay is typically out of equilibrium.

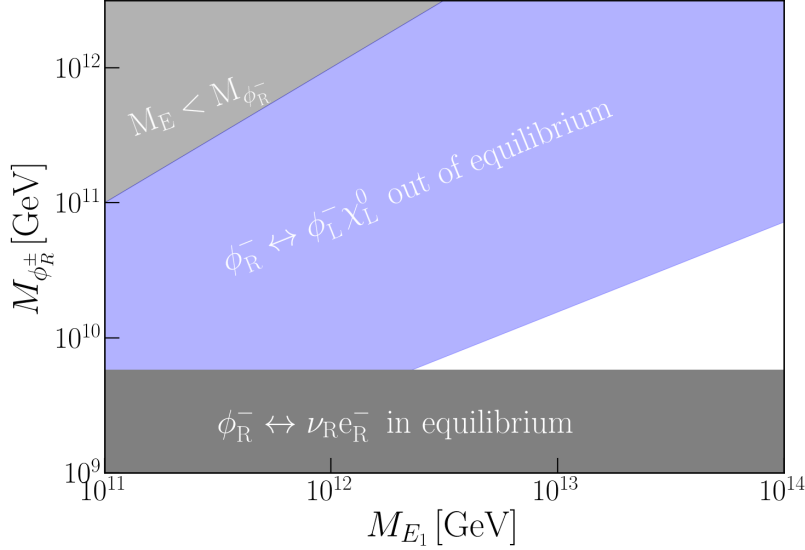


Figure 4. We show the washout process constraints in the M_E versus $M_{\phi_R^\pm}$ plane, assuming Yukawa coupling elements of f is order $f \sim 10^{-3}$ and $M_E = 0.5\kappa_R$. We require the process $\phi_R^- \rightarrow \phi_L^- \bar{\chi}_L^0$ to be in equilibrium and the process $\phi_R^- \rightarrow e_R^- \nu_R$ to be out of equilibrium. Additionally, to satisfy the perturbative unitarity condition, we require that the cubic coupling, arising from λ_5 when κ_R acquires a non-zero VEV, should not be much larger than the largest charged scalar masses $M_{\phi_R^\pm}$.

The requirements of the process $\phi_R^- \rightarrow \phi_L^- \bar{\chi}_L^0$ be in equilibrium and $\phi_R^- \rightarrow e_R^- \nu_R$ be in out-of-equilibrium provide stringent constraints to the model parameters. In the Fig. 4, we illustrate these constraints in the M_{E_1} versus $M_{\phi_R^\pm}$ plane, by assuming $M_{\phi_R^\pm} \approx M_{h_2^\pm}$, $M_E = 0.5\kappa_R$ and the elements of Yukawa coupling f are of order 10^{-3} . In addition to washout conditions, the perturbative unitarity condition requires the cubic coupling arising from λ_5 when κ_R acquires a non-zero VEV, should not be much larger than the largest charged scalar masses and here we require it to be less than $3M_{\phi_R^\pm}$. These conditions restrict the mass of heavy Dirac leptons to be roughly $M_E > 10^{12}$ GeV. The mass of E_i can be lowered down in the case of degenerate heavy leptons, utilizing the resonant enhancement of CP asymmetry. The resonant leptogenesis scenario will be discussed in more detail in Sec. 5. For a given M_E , the upper bound on $M_{\phi_R^-}$ is set by the condition that the process $\phi_R^- \rightarrow \phi_L^- \bar{\chi}_L^0$ remains in equilibrium, while the lower bound is obtained by ensuring that $\phi_R^- \rightarrow e_R^- \nu_R$ remains out of equilibrium. Additionally, we require the decay rate $\Gamma(\phi_L^- \rightarrow \psi_L \psi_L \bar{\chi}_L) > H(T)|_{T=T_{\text{sph}}}$, where $T_{\text{sph}} = 131.7 \pm 2.3$ GeV [55] is the sphaleron decoupling temperature. This condition ensures the asymmetry in ϕ_L^- is efficiently transferred to SM leptons before electroweak symmetry breaking.

In this model, $B-L$ is conserved, and we have the asymmetry $Y_{\Delta(B-L_{\text{SM}})} = Y_{\Delta\nu_R}$. The electroweak sphaleron will convert $B-L_{\text{SM}}$ asymmetry into baryon asymmetry [13, 56],

$$Y_{\Delta B} = \frac{28}{79} Y_{\Delta(B-L_{\text{SM}})} = \frac{28}{79} Y_{\Delta\nu_R}. \quad (4.28)$$

The observed baryon to entropy ratio is given by $Y_{\Delta B} = (8.579 \pm 0.109) \times 10^{-11}$ [1].

Benchmark Points			
	BP1	BP2	BP3
M_E [GeV]	$\text{diag}(3, 6, 9) \times 10^{12}$	$\text{diag}(3, 7, 11) \times 10^{12}$	$\text{diag}(4, 6, 11) \times 10^{12}$
θ_{\pm}	2.8699×10^{-10}	3.2619×10^{-10}	-9.1252×10^{-10}
$\sin^2 \theta_{12}$	0.3070	0.3070	0.3080
$\sin^2 \theta_{13}$	0.0220	0.0220	0.0222
$\sin^2 \theta_{23}$	0.5720	0.5720	0.5620
δ_{CP}	196.9945°	196.9907°	284.9969
$\Delta m_{21}^2 [10^{-5} \text{eV}]$	7.4244	7.4100	7.4900
$\Delta m_{31}^2 [10^{-3} \text{eV}]$ [NO]	2.5110	2.5159	-
$\Delta m_{23}^2 [10^{-3} \text{eV}]$ [IO]	-	-	2.5100
$Y_{\Delta B}$	8.5790×10^{-11}	8.5790×10^{-11}	8.5790×10^{-11}
χ^2	9.34×10^{-3}	7.24×10^{-8}	1.05×10^{-7}

Table I. Three benchmark point fit for the neutrino oscillation data and baryon asymmetry in the model by fixing $\kappa_R = 10^{13}$ GeV, $m_{h_2^\pm} = 10^9$ GeV and $m_{h_1^\pm} = 10^7$ GeV. Here NO and IO refer to the normal and inverted orderings of neutrino masses.

4.1 Results

To fit the neutrino oscillation data and baryon asymmetry, we perform a χ^2 -function minimization, where the χ^2 -function is defined as

$$\chi^2 = \sum_{\text{all observables}} \left(\frac{\text{theoretical predictions} - \text{experimental central value}}{\text{experimental } 1\sigma \text{ error}} \right)^2. \quad (4.29)$$

The model can give excellent fits to neutrino oscillation [57] data and baryon asymmetry for approximately $\kappa_R > 10^{13}$ GeV, as illustrated in Tab. I. This limit primarily comes from the requirement of the process $\phi_R^- \rightarrow e_R^- \nu_R$ to be out of equilibrium which requires approximately $M_{\phi_R^-} > 10^9$ GeV. This constrain can be alleviated in the resonant leptogenesis regime, which allows the scale of Yukawa coupling f to even lower and could keep the process $\phi_R^- \rightarrow e_R^- \nu_R$ out of equilibrium for lower values of $M_{\phi_R^-}$. In Tab. I, we provide benchmark points by fixing $\kappa_R = 10^{13}$ GeV, $m_{h_2} = 10^9$ GeV and $m_{h_1} = 10^7$ GeV. Here, we assume the $M_{\phi_R^-} \approx M_{h_2}$ and $M_{\phi_L^-} \approx M_{h_1}$. The benchmark points BP1 and BP2 correspond to normal ordering (NO), while BP3 corresponds to inverted ordering (IO) of neutrino masses. The Yukawa coupling matrices associated with the benchmark points are provided in Appendix A.

In Fig. 5, we present the evolution of the number densities of Dirac leptons $Y_{\Sigma E_1}$ (left panel) and the asymmetries $Y_{\Delta \nu_R}$, $Y_{\Delta e_R}$, $Y_{\Delta \psi_L}$, and $Y_{\Delta E_1}$ (right panel), obtained by solving the Boltzmann equations in Eq. (4.21). The asymmetries of $Y_{\Delta \nu_R}$, $Y_{\Delta e_R}$ and, $Y_{\Delta \psi_L}$ are almost of the same order because the CP asymmetries of the corresponding channels are of similar order. The asymmetry of $Y_{\Delta E_1}$ is significantly small compared to other asymmetries because the sum of CP violation of all decay channels of E_1 vanishes. In the weak washout regime, the asymmetries do not undergo significant washout. In this scale, the contributions

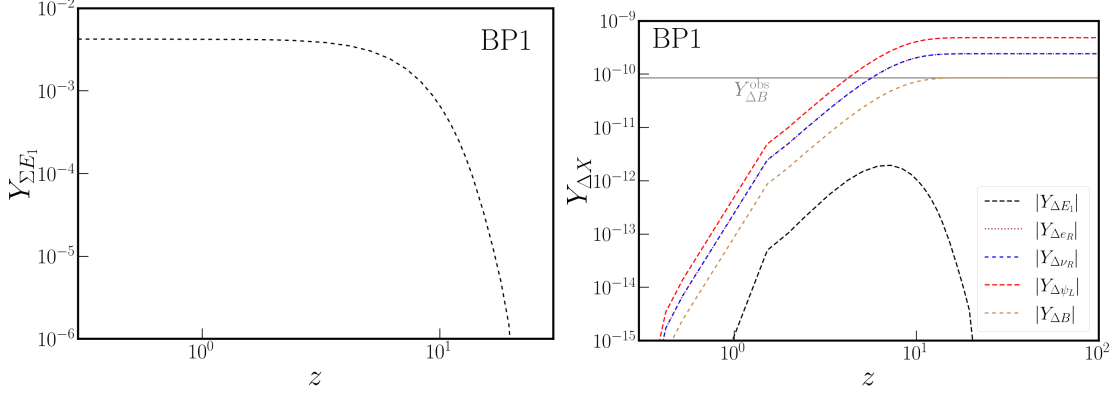


Figure 5. The evolution of number densities of Dirac leptons $Y_{\Sigma E_1}$ (left panel) and asymmetries $Y_{\Delta \nu_R}$, $Y_{\Delta e_R}$, $Y_{\Delta \psi_L}$ and $Y_{\Delta E_1}$ (right panel) obtained by solving Boltzman equations of Eq. (4.21).

from the heavier Dirac states E_2 and E_3 are negligible, as their CP violation is minimal and does not substantially impact the washout of the ν_R asymmetry. This model can give an excellent fit for neutrino oscillation data and explain the observed baryon asymmetry but with right-hand breaking scale κ_R to be approximately above 10^{13} GeV. However, this scale can be lowered using resonant enhancement of CP asymmetry, as discussed in Sec. 5.

5 Resonant Leptogenesis

The CP asymmetry can be resonantly enhanced due to the mixing of nearly degenerate heavy Dirac states having mass differences similar order to their decay widths [58]. This enhancement in CP asymmetry opens a pathway to reproduce the observed baryon asymmetry with smaller values of the f Yukawa coupling, thereby lowering the required scale of κ_R . In this scenario, the CP asymmetry generated due to the decay of \hat{E}_1 is provided by [58, 59]:

$$\epsilon_{\nu_R \phi_R^-}^1 = \frac{\text{Im} \left[(f_R^\dagger f_R)_{21} (\mathcal{Y}_L^\dagger \mathcal{Y}_L)_{12} \right] \Lambda (M_{E_1}, M_{E_2}, \Gamma_2)}{\left[(f_L^\dagger f_L)_{11} + (f_R^\dagger f_R)_{11} + (\mathcal{Y}_L^\dagger \mathcal{Y}_L)_{11} \right] \left[(f_L^\dagger f_L)_{22} + (f_R^\dagger f_R)_{22} + (\mathcal{Y}_L^\dagger \mathcal{Y}_L)_{22} \right]}, \quad (5.1)$$

$$\epsilon_{e_R^+ \phi_R^-}^1 = \frac{\text{Im} \left[(f_R^\dagger f_R)_{21} (\mathcal{Y}_L^\dagger \mathcal{Y}_L)_{12} \right] \Lambda (M_{E_1}, M_{E_2}, \Gamma_2)}{\left[(f_L^\dagger f_L)_{11} + (f_R^\dagger f_R)_{11} + (\mathcal{Y}_L^\dagger \mathcal{Y}_L)_{11} \right] \left[(f_L^\dagger f_L)_{22} + (f_R^\dagger f_R)_{22} + (\mathcal{Y}_L^\dagger \mathcal{Y}_L)_{22} \right]}, \quad (5.2)$$

$$\epsilon_{\psi_L \bar{\chi}_L}^1 = \frac{2 \text{Im} \left[(\mathcal{Y}_L^\dagger \mathcal{Y}_L)_{21} (f_R^\dagger f_R)_{12} \right] \Lambda (M_{E_1}, M_{E_2}, \Gamma_2)}{\left[(f_L^\dagger f_L)_{11} + (f_R^\dagger f_R)_{11} + (\mathcal{Y}_L^\dagger \mathcal{Y}_L)_{11} \right] \left[(f_L^\dagger f_L)_{22} + (f_R^\dagger f_R)_{22} + (\mathcal{Y}_L^\dagger \mathcal{Y}_L)_{22} \right]}, \quad (5.3)$$

Resonant Leptogenesis-Benchmark Points			
	BP4	BP5	BP6
κ_R [GeV]	10^7	10^6	10^7
$m_{h_2^\pm}$ [GeV]	10^5	8×10^4	9×10^5
$m_{h_1^\pm}$ [GeV]	7×10^4	3×10^4	4×10^5
θ_\pm	-1.3670×10^{-5}	-0.00018	3.4745×10^{-6}
$\sin^2 \theta_{12}$	0.3064	0.2920	0.3075
$\sin^2 \theta_{13}$	0.02202	0.02280	0.02201
$\sin^2 \theta_{23}$	0.5726	0.5460	0.5680
δ_{CP}	178.009°	82.091°	47.186°
$\Delta m_{21}^2 [10^{-5} \text{eV}]$	7.4095	7.3572	7.4146
$\Delta m_{31}^2 [10^{-3} \text{eV}]$	2.5117	2.5021	2.5098
$Y_{\Delta B}$	8.5789×10^{-11}	8.6983×10^{-11}	8.5789×10^{-11}
χ^2	0.0839	4.664	5.1635

Table II. Three benchmark points that for the neutrino oscillation data and baryon asymmetry in the resonant leptogenesis scenario. Here we have fixed $M_{E_3} = \kappa_R$.

where the factor $\Lambda(M_{E_1}, M_{E_2}, \Gamma_2)$ is given by

$$\Lambda(M_{E_1}, M_{E_2}, \Gamma_2) = \frac{(M_{E_2}^2 - M_{E_1}^2) M_{E_1} \Gamma_2}{(M_{E_2}^2 - M_{E_1}^2)^2 + M_{E_1}^2 \Gamma_2^2}. \quad (5.4)$$

Similarly, the CP asymmetry of \hat{E}_2 decay can be written by interchanging the indices $1 \leftrightarrow 2$. The Boltzmann equation in this scenario can be obtained by including of decay and washout of \hat{E}_2 contribution to Eq. (4.21).

Achieving a resonant scenario with a diagonal bare mass matrix M_E may appear to be significantly fine-tuned. This conclusion is, however, not basis-invariant. In this work, we consider the bare matrix M_E to be non-diagonal and for simplicity, we consider a two-family mixing scenario where the off-diagonal elements M_{12} and M_{21} are significantly larger than the diagonal elements M_{11} and M_{22} of the bare mass matrix M_E . Owing to parity symmetry we have $M_{12} = M_{21}^*$. This parametrization of the bare mass matrix would lead to the squared masses of the eigenvalues being nearly degenerate. The parametrization of Yukawa matrix \mathcal{Y}_ℓ with $\mathcal{Y}_{\ell 11}, \mathcal{Y}_{\ell 12} \ll \mathcal{Y}_{\ell 21}, \mathcal{Y}_{\ell 22}$ can also can fit the electron and muon masses.

In Fig. 6, we show the constraints arising from washout conditions in the M_{E_1} versus $M_{\phi_R^\pm}$ plane, by fixing elements of Yukawa couplings $f \approx 1.5 \times 10^{-5}$ and taking $M_E = 0.5\kappa_R$. The value of f is chosen to be as small as possible while explaining the correct baryon asymmetry utilizing resonant enhancement. The requirement of the process with $\phi_R^- \rightarrow e_R^- \nu_R$ to be out of equilibrium imposes stringent constraints. Meanwhile, the condition for the process $\phi_R^- \rightarrow \phi_L^- \bar{\chi}_L^0$ to be in equilibrium is easily satisfied for the relevant parameter space. In Tab. II, we provide the benchmark fit for the neutrino oscillation data and baryon asymmetry by fixing $M_{E_3} = \kappa_R$. As in the previous section, we

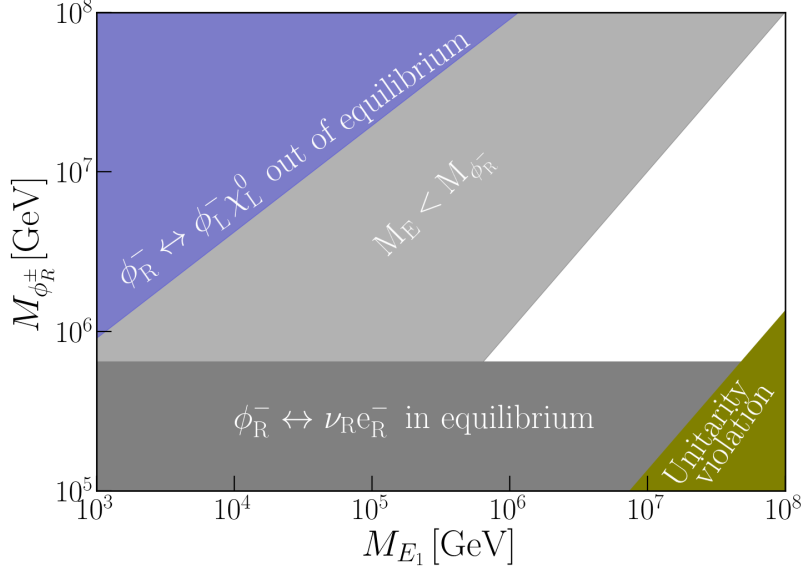


Figure 6. We show the washout process constraints in the M_{E_1} versus $M_{\phi_R^\pm}$ plane for the resonant leptogenesis scenario, assuming the Yukawa coupling elements of f is order $f \sim 1.5 \times 10^{-5}$ and $M_{E_1} = 0.5\kappa_R$. The requirement of the process with $\phi_R^- \rightarrow e_R^- \nu_R$ to be out of equilibrium provides significant constraint. Meanwhile, the process $\phi_R^- \rightarrow \phi_L^- \bar{\chi}_L^0$ is in equilibrium for all the relevant parameter space. The unitarity condition provides the lower bound for $M_{\phi_R^-}$ mass for large values of M_{E_1} .

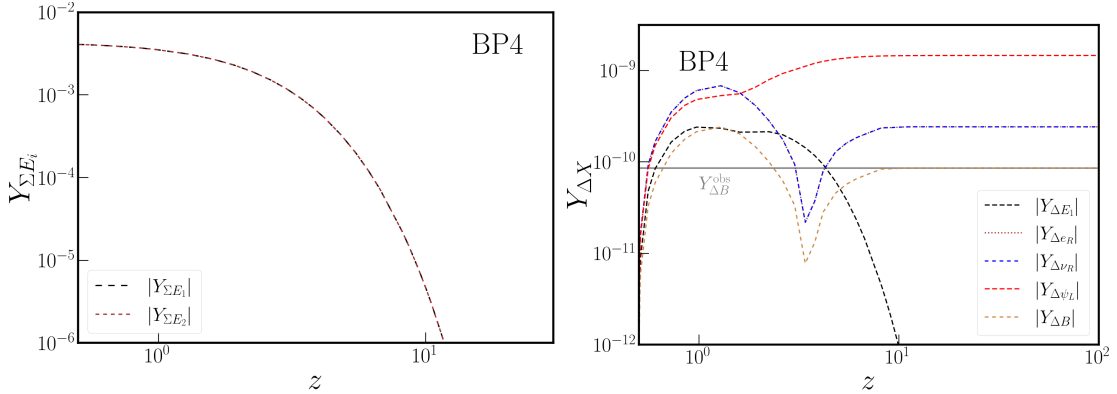


Figure 7. The evolution of number densities of Dirac leptons $Y_{\Sigma E_1}$ and $Y_{\Sigma E_2}$ (left panel) and asymmetries $Y_{\Delta \nu_R}$, $Y_{\Delta e_R}$, $Y_{\Delta \psi_L}$, $Y_{\Delta E_1}$ (right panel) obtained by solving Boltzman equations of Eq. (4.21).

assume $M_{\phi_R^-} \approx M_{h_2}$ and $M_{\phi_L^-} \approx M_{h_1}$. In this scenario, the right-handed breaking scale κ_R can be lowered to approximately 10^6 GeV. The Yukawa coupling matrices and bare mass matrices for the benchmark points in Tab.II are provided in Appendix A. In this case the model has parameter space that can solve strong CP problems evading the quality problem arising from Planck-suppressed operators [60]. In Fig. 7, we provide the evolution of asymmetries and number density of heavy Dirac state E_i as a function of $z = \hat{M}_{E_1}/T$ for

the benchmark point BP4. The asymmetry in $Y_{\Delta\nu_R}$ undergoes significant washout when $Y_{\Delta E_i} \sim Y_{\Delta\nu_R}$. Hence, the resonant enhancement of asymmetry allows a large parameter space to simultaneously explain baryon asymmetry and neutrino oscillation data in the model with right-hand breaking scale κ_R as low as 10^6 GeV.

6 Summary

We have presented in this paper a novel way of generating baryon asymmetry of the Universe via Dirac leptogenesis. The model presented is based on the left-right symmetric gauge group with a generalized seesaw mechanism inducing all charged fermion masses. Thus, the electron mass arises via mixing with a vector-like electron (E) field. Neutrinos are naturally Dirac fermions with small masses, since they do not have vector-like partners to mix with and therefore do not acquire tree-level masses. Loop diagrams involving charged scalars and the vector-like lepton field will induce finite and small Dirac neutrino masses. The decay of $E \rightarrow \bar{\nu}_R \phi_R^-$ generates a ν_R asymmetry at early times in the evolution of the Universe, which is accompanied by an equal and opposite ϕ_R^- asymmetry. This ϕ_R^- asymmetry is converted in a second stage to ϕ_L^- asymmetry which in turn is transferred to standard model lepton asymmetry.

We have identified parameter space of the model where Dirac leptogenesis and excellent fits to neutrino oscillation data are simultaneously reproduced. Typically this requires the W_R^\pm gauge boson mass to exceed 10^{13} GeV. However, we have also shown that a resonant enhancement is possible for the CP asymmetry quite naturally, in which case the W_R^\pm mass can be as low as 10^6 GeV. Since the model setup is motivated independently from a solution to the strong CP problem via parity symmetry without needing the axion, it is interesting that the low W_R^\pm scale can also protect the parity solution from Planck suppressed operators.

Acknowledgments

The work of KSB and AK are supported in part by US Department of Energy Grant Number DE-SC 0016013. We thank Ritu Dcruz and Rabi Mohapatra for helpful discussions.

A Yukawa Matrices for benchmark points

A.1 Non-resonant leptogenesis

In this section, we provide the Yukawa matrices for the benchmark points given in [Tab. I](#).

- Benchmark point 1

$$\mathcal{Y}_\ell = \begin{pmatrix} 9.3808 \times 10^{-4} & 1.1101 \times 10^{-5} & 9.0359 \times 10^{-6} \\ 2.6782 \times 10^{-4} & 3.0142 \times 10^{-2} & 1.1207 \times 10^{-2} \\ 4.8019 \times 10^{-4} & 4.8570 \times 10^{-2} & 3.2374 \times 10^{-2} \end{pmatrix}$$

$$+i \begin{pmatrix} 1.5804 \times 10^{-7} & 2.8662 \times 10^{-5} & 2.4682 \times 10^{-5} \\ 3.7411 \times 10^{-4} & -1.3378 \times 10^{-2} & -2.9516 \times 10^{-2} \\ 6.6206 \times 10^{-4} & -3.9877 \times 10^{-2} & -1.1349 \times 10^{-2} \end{pmatrix} \quad (\text{A.1})$$

$$f = \begin{pmatrix} 3.9316 \times 10^{-4} & 9.2171 \times 10^{-5} & -2.1828 \times 10^{-4} \\ -4.1052 \times 10^{-4} & 1.3457 \times 10^{-4} & -1.0764 \times 10^{-4} \\ 7.3347 \times 10^{-4} & -3.0002 \times 10^{-4} & 4.8038 \times 10^{-4} \end{pmatrix}$$

$$+i \begin{pmatrix} 3.3318 \times 10^{-4} & 1.8423 \times 10^{-4} & -4.4608 \times 10^{-4} \\ -1.7256 \times 10^{-3} & 6.5935 \times 10^{-4} & -1.3166 \times 10^{-3} \\ -7.2153 \times 10^{-4} & -3.1281 \times 10^{-4} & 1.0061 \times 10^{-3} \end{pmatrix} \quad (\text{A.2})$$

- Benchmark point 2

$$\mathcal{Y}_\ell = \begin{pmatrix} -9.3797 \times 10^{-4} & -1.6271 \times 10^{-5} & -1.1164 \times 10^{-5} \\ 3.3239 \times 10^{-4} & 1.7466 \times 10^{-2} & 6.9582 \times 10^{-3} \\ 7.3119 \times 10^{-4} & 3.5579 \times 10^{-2} & 2.2248 \times 10^{-2} \end{pmatrix}$$

$$+i \begin{pmatrix} -2.0532 \times 10^{-7} & -3.8928 \times 10^{-5} & -3.5515 \times 10^{-5} \\ 2.0232 \times 10^{-4} & -1.9426 \times 10^{-2} & -3.7042 \times 10^{-2} \\ 4.4132 \times 10^{-4} & -6.3230 \times 10^{-2} & -2.5120 \times 10^{-2} \end{pmatrix} \quad (\text{A.3})$$

$$f = \begin{pmatrix} 3.6433 \times 10^{-4} & -6.1492 \times 10^{-6} & -2.3051 \times 10^{-4} \\ 9.2607 \times 10^{-4} & -3.6450 \times 10^{-4} & 7.4739 \times 10^{-4} \\ -1.1937 \times 10^{-3} & 6.0756 \times 10^{-4} & -1.2539 \times 10^{-3} \end{pmatrix}$$

$$+i \begin{pmatrix} -3.6145 \times 10^{-5} & 2.8235 \times 10^{-4} & -6.8006 \times 10^{-4} \\ -7.9128 \times 10^{-4} & -1.3115 \times 10^{-4} & 7.8428 \times 10^{-4} \\ -9.1375 \times 10^{-4} & 3.2894 \times 10^{-4} & -5.1919 \times 10^{-4} \end{pmatrix} \quad (\text{A.4})$$

- Benchmark point 3

$$Y_\ell = \begin{pmatrix} -1.0832 \times 10^{-3} & -8.2140 \times 10^{-6} & -1.2928 \times 10^{-5} \\ 3.1821 \times 10^{-5} & -9.8975 \times 10^{-4} & -5.0831 \times 10^{-3} \\ -1.5283 \times 10^{-5} & -7.0477 \times 10^{-2} & -4.5838 \times 10^{-2} \end{pmatrix}$$

$$+i \begin{pmatrix} -1.7055 \times 10^{-7} & -2.9522 \times 10^{-5} & -1.0056 \times 10^{-5} \\ -8.3155 \times 10^{-5} & -8.1735 \times 10^{-3} & 2.2935 \times 10^{-2} \\ -1.0798 \times 10^{-3} & 1.6323 \times 10^{-3} & -1.5392 \times 10^{-3} \end{pmatrix} \quad (\text{A.5})$$

$$f = \begin{pmatrix} -4.8988 \times 10^{-4} & 4.7672 \times 10^{-4} & -1.1106 \times 10^{-3} \\ -7.3062 \times 10^{-4} & -3.2052 \times 10^{-4} & 8.3238 \times 10^{-4} \\ -3.2292 \times 10^{-4} & 6.9002 \times 10^{-5} & -1.1048 \times 10^{-4} \end{pmatrix}$$

$$+i \begin{pmatrix} -7.8634 \times 10^{-4} & 3.4455 \times 10^{-4} & -1.0200 \times 10^{-3} \\ -1.6813 \times 10^{-4} & -6.8320 \times 10^{-5} & 2.3417 \times 10^{-4} \\ 7.2470 \times 10^{-4} & 1.9106 \times 10^{-4} & -1.1476 \times 10^{-3} \end{pmatrix} \quad (\text{A.6})$$

A.2 Resonant leptogenesis

In this section, we provide the Yukawa matrices and bare mass matrix for heavy leptons for the benchmark points given in [Tab. II](#).

- Benchmark point 4

$$M_E = \begin{pmatrix} -3.5127 \times 10^3 & 5.0000 \times 10^6 & 0 \\ 5.0000 \times 10^6 & 5.0513 \times 10^2 & 0 \\ 0 & 0 & 1.0000 \times 10^7 \end{pmatrix} \quad (\text{A.7})$$

$$Y_\ell = \begin{pmatrix} 9.2266 \times 10^{-3} & 1.4909 \times 10^{-2} & 0 \\ 3.5637 \times 10^{-3} & 3.5337 \times 10^{-3} & 0 \\ 0 & 0 & 1.0102 \times 10^{-1} \end{pmatrix} \\ +i \begin{pmatrix} -5.5485 \times 10^{-3} & 7.9198 \times 10^{-4} & 0 \\ 1.7335 \times 10^{-3} & 2.9641 \times 10^{-3} & 0 \\ 0 & 0 & 0 \end{pmatrix} \quad (\text{A.8})$$

$$f = \begin{pmatrix} 8.5526 \times 10^{-7} & -3.2444 \times 10^{-5} & 3.5315 \times 10^{-6} \\ 7.9091 \times 10^{-6} & -4.6937 \times 10^{-6} & 6.4085 \times 10^{-7} \\ 2.5420 \times 10^{-5} & -9.9093 \times 10^{-7} & -4.3673 \times 10^{-7} \end{pmatrix} \\ +i \begin{pmatrix} 1.0152 \times 10^{-5} & -8.2403 \times 10^{-6} & -5.0696 \times 10^{-6} \\ 1.2359 \times 10^{-5} & -9.4696 \times 10^{-6} & -3.0909 \times 10^{-6} \\ -4.5565 \times 10^{-6} & 1.9182 \times 10^{-5} & 7.2618 \times 10^{-6} \end{pmatrix} \quad (\text{A.9})$$

- Benchmark point 5

$$M_E = \begin{pmatrix} 6.4577 \times 10^2 & 8.0000 \times 10^5 & 0 \\ 8.0000 \times 10^5 & -9.4179 \times 10^2 & 0 \\ 0 & 0 & 1.0000 \times 10^6 \end{pmatrix} \quad (\text{A.10})$$

$$Y_\ell = \begin{pmatrix} 7.7557 \times 10^{-3} & 3.7269 \times 10^{-3} & 0 \\ 1.4150 \times 10^{-2} & 4.1527 \times 10^{-3} & 0 \\ 0 & 0 & 1.0102 \times 10^{-1} \end{pmatrix} \\ +i \begin{pmatrix} 2.0838 \times 10^{-2} & 6.5795 \times 10^{-3} & 0 \\ 6.3805 \times 10^{-3} & 2.5708 \times 10^{-3} & 0 \\ 0 & 0 & 0 \end{pmatrix} \quad (\text{A.11})$$

$$f = \begin{pmatrix} 1.8701 \times 10^{-5} & 7.7064 \times 10^{-6} & 6.9872 \times 10^{-7} \\ 1.4562 \times 10^{-5} & 7.1015 \times 10^{-6} & -6.9614 \times 10^{-6} \\ -2.7149 \times 10^{-5} & -1.4744 \times 10^{-5} & -1.6045 \times 10^{-7} \end{pmatrix} \\ +i \begin{pmatrix} 1.9352 \times 10^{-5} & -1.2240 \times 10^{-5} & -3.9548 \times 10^{-6} \\ 6.5784 \times 10^{-6} & 9.7436 \times 10^{-7} & -3.2886 \times 10^{-7} \\ 5.8198 \times 10^{-6} & -1.8853 \times 10^{-6} & -2.4888 \times 10^{-6} \end{pmatrix} \quad (\text{A.12})$$

- Benchmark point 6

$$M_E = \begin{pmatrix} -9.0603 \times 10^3 & 7.0000 \times 10^6 & 0 \\ 7.0000 \times 10^6 & 5.9828 \times 10^3 & 0 \\ 0 & 0 & 1.0000 \times 10^7 \end{pmatrix} \quad (\text{A.13})$$

$$Y_\ell = \begin{pmatrix} 2.1359 \times 10^{-3} & 1.2788 \times 10^{-3} & 0 \\ 1.5337 \times 10^{-3} & 3.4215 \times 10^{-4} & 0 \\ 0 & 0 & 1.0102 \times 10^{-1} \end{pmatrix}$$

$$+i \begin{pmatrix} 2.8843 \times 10^{-2} & 7.2485 \times 10^{-3} & 0 \\ 3.4440 \times 10^{-3} & -1.7980 \times 10^{-4} & 0 \\ 0 & 0 & 0 \end{pmatrix} \quad (\text{A.14})$$

$$f = \begin{pmatrix} 6.0894 \times 10^{-5} & 1.1534 \times 10^{-5} & 4.7117 \times 10^{-7} \\ -2.9089 \times 10^{-6} & 1.6570 \times 10^{-5} & -3.4130 \times 10^{-6} \\ 4.2229 \times 10^{-5} & 3.2230 \times 10^{-5} & -3.0666 \times 10^{-6} \end{pmatrix}$$

$$+i \begin{pmatrix} 2.7605 \times 10^{-6} & -1.1476 \times 10^{-5} & -6.6157 \times 10^{-8} \\ 8.2524 \times 10^{-6} & 5.8244 \times 10^{-6} & -5.3561 \times 10^{-6} \\ -1.2857 \times 10^{-5} & 1.5163 \times 10^{-5} & 1.4178 \times 10^{-6} \end{pmatrix} \quad (\text{A.15})$$

References

- [1] **Planck** Collaboration, N. Aghanim *et al.*, “Planck 2018 results. VI. Cosmological parameters,” *Astron. Astrophys.* **641** (2020) A6, [arXiv:1807.06209 \[astro-ph.CO\]](#). [Erratum: *Astron. Astrophys.* 652, C4 (2021)].
- [2] R. Davis, “A review of the homestake solar neutrino experiment,” *Progress in Particle and Nuclear Physics* **32** (1994) 13–32. <https://api.semanticscholar.org/CorpusID:122658718>.
- [3] **Super-Kamiokande** Collaboration, Y. Fukuda *et al.*, “Evidence for oscillation of atmospheric neutrinos,” *Phys. Rev. Lett.* **81** (1998) 1562–1567, [arXiv:hep-ex/9807003](#).
- [4] **SNO** Collaboration, Q. R. Ahmad *et al.*, “Direct evidence for neutrino flavor transformation from neutral current interactions in the Sudbury Neutrino Observatory,” *Phys. Rev. Lett.* **89** (2002) 011301, [arXiv:nucl-ex/0204008](#).
- [5] **Daya Bay** Collaboration, F. P. An *et al.*, “Observation of electron-antineutrino disappearance at Daya Bay,” *Phys. Rev. Lett.* **108** (2012) 171803, [arXiv:1203.1669 \[hep-ex\]](#).
- [6] M. J. Dolinski, A. W. P. Poon, and W. Rodejohann, “Neutrinoless Double-Beta Decay: Status and Prospects,” *Ann. Rev. Nucl. Part. Sci.* **69** (2019) 219–251, [arXiv:1902.04097 \[nucl-ex\]](#).
- [7] P. Minkowski, “ $\mu \rightarrow e\gamma$ at a Rate of One Out of 10^9 Muon Decays?,” *Phys. Lett. B* **67** (1977) 421–428.
- [8] T. Yanagida, “Horizontal gauge symmetry and masses of neutrinos,” *Conf. Proc. C* **7902131** (1979) 95–99.
- [9] S. L. Glashow, “The Future of Elementary Particle Physics,” *NATO Sci. Ser. B* **61** (1980) 687.

- [10] M. Gell-Mann, P. Ramond, and R. Slansky, “Complex Spinors and Unified Theories,” *Conf. Proc. C* **790927** (1979) 315–321, [arXiv:1306.4669 \[hep-th\]](#).
- [11] R. N. Mohapatra and G. Senjanovic, “Neutrino Mass and Spontaneous Parity Nonconservation,” *Phys. Rev. Lett.* **44** (1980) 912.
- [12] M. Fukugita and T. Yanagida, “Baryogenesis Without Grand Unification,” *Phys. Lett. B* **174** (1986) 45–47.
- [13] V. A. Kuzmin, V. A. Rubakov, and M. E. Shaposhnikov, “On the Anomalous Electroweak Baryon Number Nonconservation in the Early Universe,” *Phys. Lett. B* **155** (1985) 36.
- [14] S. Davidson, E. Nardi, and Y. Nir, “Leptogenesis,” *Phys. Rept.* **466** (2008) 105–177, [arXiv:0802.2962 \[hep-ph\]](#).
- [15] K. Dick, M. Lindner, M. Ratz, and D. Wright, “Leptogenesis with Dirac neutrinos,” *Phys. Rev. Lett.* **84** (2000) 4039–4042, [arXiv:hep-ph/9907562](#).
- [16] H. Murayama and A. Pierce, “Realistic Dirac leptogenesis,” *Phys. Rev. Lett.* **89** (2002) 271601, [arXiv:hep-ph/0206177](#).
- [17] M. Boz and N. K. Pak, “Dirac Leptogenesis and anomalous U(1),” *Eur. Phys. J. C* **37** (2004) 507–510.
- [18] B. Thomas and M. Toharia, “Phenomenology of Dirac neutrino genesis in split supersymmetry,” *Phys. Rev. D* **73** (2006) 063512, [arXiv:hep-ph/0511206](#).
- [19] D. G. Cerdeno, A. Dedes, and T. E. J. Underwood, “The Minimal Phantom Sector of the Standard Model: Higgs Phenomenology and Dirac Leptogenesis,” *JHEP* **09** (2006) 067, [arXiv:hep-ph/0607157](#).
- [20] B. Thomas and M. Toharia, “Lepton flavor violation and supersymmetric Dirac leptogenesis,” *Phys. Rev. D* **75** (2007) 013013, [arXiv:hep-ph/0607285](#).
- [21] P.-H. Gu and H.-J. He, “Neutrino Mass and Baryon Asymmetry from Dirac Seesaw,” *JCAP* **12** (2006) 010, [arXiv:hep-ph/0610275](#).
- [22] P.-H. Gu, H.-J. He, and U. Sarkar, “Realistic neutrino genesis with radiative vertex correction,” *Phys. Lett. B* **659** (2008) 634–639, [arXiv:0709.1019 \[hep-ph\]](#).
- [23] E. J. Chun and P. Roy, “Dirac Leptogenesis in extended nMSSM,” *JHEP* **06** (2008) 089, [arXiv:0803.1720 \[hep-ph\]](#).
- [24] A. Bechinger and G. Seidl, “Resonant Dirac leptogenesis on throats,” *Phys. Rev. D* **81** (2010) 065015, [arXiv:0907.4341 \[hep-ph\]](#).
- [25] D. Borah and A. Dasgupta, “Common Origin of Neutrino Mass, Dark Matter and Dirac Leptogenesis,” *JCAP* **12** (2016) 034, [arXiv:1608.03872 \[hep-ph\]](#).
- [26] K. Earl, C. S. Fong, T. Gregoire, and A. Tonero, “Mirror Dirac leptogenesis,” *JCAP* **03** (2020) 036, [arXiv:1903.12192 \[hep-ph\]](#).
- [27] J. Heck, J. Heisig, and A. Thapa, “Testing Dirac leptogenesis with the cosmic microwave background and proton decay,” *Phys. Rev. D* **108** no. 3, (2023) 035014, [arXiv:2304.09893 \[hep-ph\]](#).
- [28] J. C. Pati and A. Salam, “Lepton Number as the Fourth Color,” *Phys. Rev. D* **10** (1974) 275–289. [Erratum: *Phys.Rev.D* 11, 703–703 (1975)].

- [29] R. N. Mohapatra and J. C. Pati, “Left-Right Gauge Symmetry and an Isoconjugate Model of CP Violation,” *Phys. Rev. D* **11** (1975) 566–571.
- [30] R. N. Mohapatra and J. C. Pati, “A Natural Left-Right Symmetry,” *Phys. Rev. D* **11** (1975) 2558.
- [31] G. Senjanovic and R. N. Mohapatra, “Exact Left-Right Symmetry and Spontaneous Violation of Parity,” *Phys. Rev. D* **12** (1975) 1502.
- [32] R. N. Mohapatra and G. Senjanovic, “Neutrino Masses and Mixings in Gauge Models with Spontaneous Parity Violation,” *Phys. Rev. D* **23** (1981) 165.
- [33] Z. G. Berezhiani, “The Weak Mixing Angles in Gauge Models with Horizontal Symmetry: A New Approach to Quark and Lepton Masses,” *Phys. Lett. B* **129** (1983) 99–102.
- [34] A. Davidson and K. C. Wali, “Universal Seesaw Mechanism?,” *Phys. Rev. Lett.* **59** (1987) 393.
- [35] S. Rajpoot, “See-saw masses for quarks and leptons in an ambidextrous electroweak interaction model,” *Mod. Phys. Lett. A* **2** no. 5, (1987) 307–315. [Erratum: *Mod.Phys.Lett.A* **2**, 541 (1987)].
- [36] K. S. Babu and R. N. Mohapatra, “CP Violation in Seesaw Models of Quark Masses,” *Phys. Rev. Lett.* **62** (1989) 1079.
- [37] K. S. Babu and R. N. Mohapatra, “A Solution to the Strong CP Problem Without an Axion,” *Phys. Rev. D* **41** (1990) 1286.
- [38] K. S. Babu and X. G. He, “Dirac neutrino masses as two loop radiative corrections,” *Mod. Phys. Lett. A* **4** (1989) 61.
- [39] K. S. Babu, X.-G. He, M. Su, and A. Thapa, “Naturally light Dirac and pseudo-Dirac neutrinos from left-right symmetry,” *JHEP* **08** (2022) 140, [arXiv:2205.09127 \[hep-ph\]](#).
- [40] R. N. Mohapatra, “Left-right Symmetry and Finite One Loop Dirac Neutrino Mass,” *Phys. Lett. B* **201** (1988) 517–524.
- [41] K. S. Babu, R. N. Mohapatra, and A. Thapa, “Predictive Dirac neutrino spectrum with strong CP solution in $SU(5)_L \times SU(5)_R$ unification,” *JHEP* **04** (2024) 049, [arXiv:2312.14096 \[hep-ph\]](#).
- [42] T. Banno, J. Hisano, T. Kitahara, and N. Osamura, “Closer look at the matching condition for radiative QCD θ parameter,” *JHEP* **02** (2024) 195, [arXiv:2311.07817 \[hep-ph\]](#).
- [43] J. de Vries, P. Draper, and H. H. Patel, “Do Minimal Parity Solutions to the Strong CP Problem Work?,” [arXiv:2109.01630 \[hep-ph\]](#).
- [44] N. Craig, I. Garcia Garcia, G. Koszegi, and A. McCune, “P not PQ,” *JHEP* **09** (2021) 130, [arXiv:2012.13416 \[hep-ph\]](#).
- [45] R. Dcruz and K. S. Babu, “Resolving W boson mass shift and CKM unitarity violation in left-right symmetric models with a universal seesaw mechanism,” *Phys. Rev. D* **108** no. 9, (2023) 095011, [arXiv:2212.09697 \[hep-ph\]](#).
- [46] R. Dcruz, “Flavor physics constraints on left-right symmetric models with universal seesaw,” *Nucl. Phys. B* **1001** (2024) 116519, [arXiv:2301.10786 \[hep-ph\]](#).
- [47] S. Jana, S. Klett, and M. Lindner, “Flavor seesaw mechanism,” *Phys. Rev. D* **105** no. 11, (2022) 115015, [arXiv:2112.09155 \[hep-ph\]](#).

- [48] D. Borah and A. Dasgupta, “Naturally Light Dirac Neutrino in Left-Right Symmetric Model,” *JCAP* **06** (2017) 003, [arXiv:1702.02877 \[hep-ph\]](#).
- [49] R. N. Mohapatra, “Left-right symmetry and finite one-loop dirac neutrino mass,” *Physics Letters B* **201** (1988) 517–524.
- [50] L. Gráf, S. Jana, A. Kaladharan, and S. Saad, “Gravitational wave imprints of left-right symmetric model with minimal Higgs sector,” *JCAP* **05** no. 05, (2022) 003, [arXiv:2112.12041 \[hep-ph\]](#).
- [51] S. P. Maharathy, M. Mitra, and A. Sarkar, “An alternate left-right symmetric model with Dirac neutrinos,” *Eur. Phys. J. C* **83** no. 6, (2023) 480, [arXiv:2211.09675 \[hep-ph\]](#).
- [52] Y. Farzan and E. Ma, “Dirac neutrino mass generation from dark matter,” *Phys. Rev. D* **86** (Aug, 2012) 033007. <https://link.aps.org/doi/10.1103/PhysRevD.86.033007>.
- [53] A. Zee, “A theory of lepton number violation and neutrino majorana masses,” *Physics Letters B* **93** no. 4, (1980) 389–393. <https://www.sciencedirect.com/science/article/pii/0370269380903494>.
- [54] E. Ma, “Verifiable radiative seesaw mechanism of neutrino mass and dark matter,” *Phys. Rev. D* **73** (2006) 077301, [arXiv:hep-ph/0601225](#).
- [55] M. D’Onofrio, K. Rummukainen, and A. Tranberg, “Sphaleron Rate in the Minimal Standard Model,” *Phys. Rev. Lett.* **113** no. 14, (2014) 141602, [arXiv:1404.3565 \[hep-ph\]](#).
- [56] J. A. Harvey and M. S. Turner, “Cosmological baryon and lepton number in the presence of electroweak fermion-number violation,” *Phys. Rev. D* **42** (Nov, 1990) 3344–3349. <https://link.aps.org/doi/10.1103/PhysRevD.42.3344>.
- [57] I. Esteban, M. C. Gonzalez-Garcia, M. Maltoni, I. Martinez-Soler, J. a. P. Pinheiro, and T. Schwetz, “NuFit-6.0: Updated global analysis of three-flavor neutrino oscillations,” [arXiv:2410.05380 \[hep-ph\]](#).
- [58] A. Pilaftsis and T. E. J. Underwood, “Resonant leptogenesis,” *Nucl. Phys. B* **692** (2004) 303–345, [arXiv:hep-ph/0309342](#).
- [59] A. Pilaftsis, “CP violation and baryogenesis due to heavy majorana neutrinos,” *Phys. Rev. D* **56** (Nov, 1997) 5431–5451. <https://link.aps.org/doi/10.1103/PhysRevD.56.5431>.
- [60] Z. G. Berezhiani, R. N. Mohapatra, and G. Senjanovic, “Planck scale physics and solutions to the strong CP problem without axion,” *Phys. Rev. D* **47** (1993) 5565–5570, [arXiv:hep-ph/9212318](#).